Measurement of spin correlation coefficients in $\vec{p}\vec{p} \rightarrow d\pi^+$

B. v. Przewoski, J. T. Balewski,* J. Doskow, H. O. Meyer, R. E. Pollock, T. Rinckel, P. Thörngren-Engblom,† and A. Wellinghausen
Department of Physics and Cyclotron Facility, Indiana University, Bloomington, Indiana 47405

W. Haeberli, B. Lorentz,‡ F. Rathmann,‡ B. Schwartz, and T. Wise
University of Wisconsin-Madison, Madison, Wisconsin 53706

W. W. Daehnick and Swapan K. Saha§
Department of Physics and Astronomy, University of Pittsburgh, Pittsburgh, Pennsylvania 15260

P. V. Pancella
Western Michigan University, Kalamazoo, Michigan 49008
(Received 16 December 1999; published 10 May 2000)

The spin correlation coefficent combinations $A_{xx}+A_{yy}$ and $A_{xx}-A_{yy}$, the spin correlation coefficients A_{xz} and A_{zz}, and the analyzing power were measured for $\vec{p}\vec{p} \rightarrow d\pi^+$ between center-of-mass angles $25° \leqslant \theta \leqslant 65°$ at beam energies of 350.5, 375.0, and 400.0 MeV. The experiment was carried out with a polarized internal target and a stored, polarized beam. Nonvertical beam polarization needed for the measurement of A_{zz} was obtained by the use of solenoidal spin rotators. Near threshold, only a few partial waves contribute, and pion *s* and *p* waves dominate with a possible small admixture of *d* waves. Certain combinations of the observables reported here are a direct measure of these *d* waves. The *d*-wave contributions are found to be negligible even at 400.0 MeV.

PACS number(s): 24.70.+s, 25.10.+s, 29.20.Dh, 29.25.Pj

I. INTRODUCTION

Over the past 50 years $NN \rightarrow NN\pi$ reactions have received considerable interest. Of those, $pp \rightarrow d\pi^+$ is probably the one which has been most extensively studied. This is because it is experimentally much easier to identify a two-particle final state. Most older measurements of this reaction are concentrated at higher energies where production via the Δ resonance dominates. With the advent of storage ring technology and internal targets the energy regime closer to threshold has become accessible. The first $NN \rightarrow NN\pi$ measurements close to threshold were restricted to cross section and analyzing power measurements [1–8], since polarized internal targets were not yet available. Measurements of spin correlation coefficients close to threshold became feasible only recently with the availability of windowless and pure polarized targets internal to storage rings [9–11].

At energies well above threshold a number of measurements of spin correlation coefficients in $pp \rightarrow d\pi^+$ exist. Of these, the ones closest to threshold are measurements of A_{zz} at 401 and 425 MeV [12] which have been performed using an external beam and a polarized target.

A parametrization in terms of partial wave amplitudes of the $pp \rightarrow d\pi^+$ data from threshold to 580 MeV was carried out by Bugg 15 years ago [13]. A more recent, updated partial-wave analysis is maintained by the Virginia group [14]. With only the cross section and the analyzing power as input, the number of free parameters is usually lowered by theoretical input such as a constraint on the phases of the amplitudes which is provided by Watson's theorem [15]. In this respect, a measurement of spin correlation parameters represents crucial new information because one can relate these observables to certain combination of amplitudes without any model assumptions.

Close to threshold, *s* and *p* wave amplitudes in the pion channel with a possible small admixture of *d* waves, are sufficient to parametrize the data. In the following, we will demonstrate that combinations of the spin correlation observables presented here are directly sensitive to the strength of these *d* waves.

II. EXPERIMENTAL ARRANGEMENT

In this paper we report measurements of spin correlation coefficients in $\vec{p}\vec{p} \rightarrow d\pi^+$ at 350.5, 375.0, and 400.0 MeV at center-of-mass angles between 25° and 65°. The experiment was carried out at the Indiana Cooler with the PINTEX[1] setup. PINTEX is located in the A region of the Indiana Cooler. In this location the dispersion almost vanishes and the horizontal and vertical betatron functions are small, al-

*Permanent address: Institute of Nuclear Physics, Cracow 31342, Poland.
†Present address: Department of Radiation Sciences, S-75121 Uppsala, Sweden.
‡Present address: Forschungs Zentrum Jülich GmbH, 52425 Jülich, Germany.
§Permanent address: Bose Institute, Calcutta 700009, India.

[1]Polarized INternal Target EXperiment.

lowing the use of a narrow target cell. The target setup consists of an atomic beam source [16] which injects polarized hydrogen atoms into the storage cell.

Vertically polarized protons from the cyclotron were stack-injected into the ring at 197 MeV, reaching an orbiting current of several 100 μA within a few minutes. The beam was then accelerated. After typically 10 min of data taking, the remaining beam was discarded, and the cycle was repeated.

The target and detector used for this experiment are the same as described in [9], and a detailed account of the apparatus can be found in [17]. The internal polarized target consisted of an open-ended 25 cm long storage cell of 12 mm diameter and 25 μm wall thickness. The cell is coated with teflon to avoid depolarization of atoms colliding with the wall. During data taking, the target polarization $\vec{Q}$ is changed every 2 s pointing in sequence, up or down ($\pm y$), left or right ($\pm x$), and along or opposite to the beam direction ($\pm z$). The magnitude of the polarization was typically $|\vec{Q}| \sim 0.75$ and is the same within ± 0.005 for all orientations [18,19].

The detector arrangement consists of a stack of scintillators and wire chambers, covering a forward cone between polar angles of 5° and 30°. From the time of flight and the relative energy deposited in the layers of the detector, the outgoing charged particles are identified as pions, protons, or deuterons. The detector system was optimized for an experiment to study the spin dependence in $\vec{p}\vec{p} \to pp\pi^0$ and $\vec{p}\vec{p} \to pn\pi^+$ near threshold [9,10]. The $\vec{p}\vec{p} \to d\pi^+$ data presented here are a by-product of that experiment.

Date were taken with vertical as well as longitudinal beam polarization. To achieve nonvertical beam polarization the proton spin was precessed by two spin-rotating solenoids located in nonadjacent sections of the six-sided Cooler. The vertical and longitudinal components of the beam polarization $\vec{P}$ at the target are about equal, with a small sideways component, while its magnitude was typically $|\vec{P}| \sim 0.6$. Since the solenoid fields are fixed in strength, the exact polarization direction depends on beam energy after acceleration. In alternating measurement cycles, the sign of the beam polarization is reversed. More details on the preparation of nonvertical beam polarization in a storage ring can be found in Ref. [19].

III. DATA ACQUISITION AND PROCESSING

For each beam polarization direction, data are acquired for all 12 possible polarization combinations of beam ($+$, $-$) and target ($\pm x, \pm y, \pm z$). The event trigger is such that two charged particles are detected in coincidence. Then, a minimum χ^2 fit to the hits in each of the four wire chamber planes is performed in order to determine how well the event conforms with a physical two-prong event that originates in the target. Events with $\chi^2 \leqslant 5$ were included in the final data sample. The information from the χ^2 fit allows us to determine the polar and azimuthal angles of both charged particles. In the case of a two-particle final state the two particles are coplanar and the expected difference between the two azimuthal angles is $\Delta\phi = 180°$. Events between $150° \leqslant \Delta\phi \leqslant 210°$ are accepted for the final analysis. The polar angles of the pion and the deuteron are correlated such that the deuteron, because of its mass, exits at angles close to the beam whereas pion laboratory angles as large as 180° are kinematically allowed. At energies below 350.5 MeV the limited acceptance of the detector setup is caused by deuterons traveling through the central hole of the detector stack, whereas at higher energies the angular coverage is more and more restricted because of π^+ missing the acceptance of 30°. Events within 1° of the predicted correlation of the π^+-d polar scattering angles were included in the final analysis. Since there is a kinematically allowed maximum deuteron angle which depends on the beam energy, only those two-prong events were included in the final data sample for which the deuteron reaction angle was $\leqslant 7°$, 8°, and 9° at 350.5, 375.0, and 400.0 MeV, respectively. The correlation between the polar angles of the pion and the deuteron and the coplanarity condition uniquely determine the $pp \to d\pi^+$ reaction channel. Therefore, the inclusion of particle identification gates in the analysis did not change the spin correlation coefficients by more than a fraction of an error bar. Consequently, no particle identification gates were used in the final analysis.

Since an open-ended storage cell is used, the target is distributed along the beam (z) axis. The resulting target density is roughly triangular extending from $z = -12$ cm to $z = +12$ cm with $z = 0$ being the location where the polarized atoms are injected. The angular acceptance of the detector depends on the origin of the event along the z axis. Specifically, the smallest detectable angle increases towards the upstream end of the cell. It was only possible to detect deuterons which originated predominatly from the upstream part of the target. Since the kinematically allowed maximum deuteron angle increases with energy, vertex coordinates between $z = -12$ cm and 4, 6, 8 cm at 350.5, 375.0, and 400.0 MeV, respectively, were accepted into the data sample. This way, background events originating from the downstream cell walls were suppressed.

The known spin correlation coefficients of proton-proton elastic scattering [20] are used to monitor beam and target polarization, concurrently with the acquisition of $pp \to d\pi^+$ events. To this end, coincidences between two protons exiting near $\Theta_{\rm lab} = 45°$ are detected by two pairs of scintillators placed behind the first wire chamber at azimuthal angles $\pm 45°$ and $\pm 135°$. From this measurement, the products $P_y Q_y$ and $P_z Q_z$ of beam and target polarization are deduced. Values for the products of beam and target polarization can be found in Table I of Ref. [11].

Background arises from reactions in the walls of the target cell and from outgassing of the teflon coating [17]. The contribution arising from a $\sim 1\%$ impurity in the target gas is negligible. Background, which is not rejected by the software cuts described above, manifests itself as a broad distribution underlying the peak at $\Delta\phi = 180°$. A measurement with a nitrogen target matches the shape of the $\Delta\phi$ distribution seen with the H target, except for the peak at 180°. This shape is used to subtract the background under the $\Delta\phi$ peak. Within statistics, the background shows no spin dependence

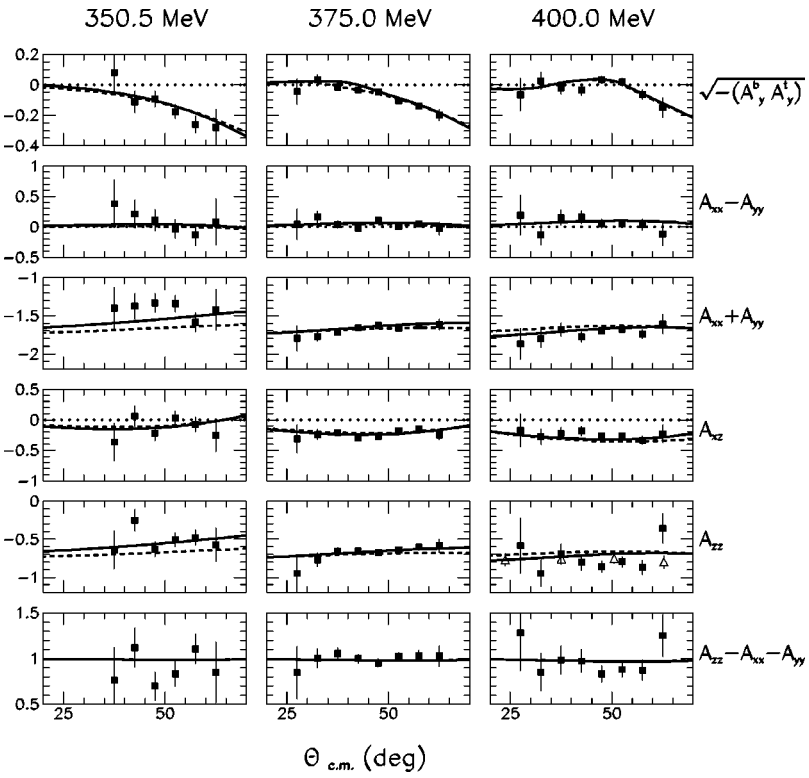

FIG. 1. Spin observables for $\vec{p}\vec{p}\to d\pi^+$. Beam and target analyzing power are taken at θ and $180°-\theta$, respectively. The open triangles are the A_{zz} measurement at 401 MeV of Ref. [12]. The solid and dashed lines are the SAID SP96 and SP93 solutions, respectively. The dotted line represents zero.

and is independent of the polar angle. The subtracted background ranges from 2% to 5%.

IV. DETERMINATION OF A_y, A_{xx}, A_{yy}, AND A_{xz}

The analyzing power and spin correlation coefficients were determined using the method of diagonal scaling. Previously, we used diagonal scaling to analyze a series of experiments to measure spin correlation coefficients in pp elastic scattering and a detailed desciption of the formalism can be found in Ref. [21].

Since we only measure the *product* of beam and target polarization $P\cdot Q$, we cannot normalize beam and target analyzing power independently. Because of the identity of the colliding particles, beam and target analyzing power as a function of center-of-mass angle are related such that $A_y^b(\theta)=-A_y^t(180°-\theta)$, in particular $A_y^b(90°)=-A_y^t(90°)$. For comparison with theory we use the quantity $\sqrt{-(A_y^b(\theta)A_y^t(\theta))}$ for which the absolute normalization depends on $P\cdot Q$ and therefore is known. The final data with their statistical errors are shown in Fig. 1.

V. PARTIAL WAVES

When one restricts the angular momentum of the pion to $l_\pi\leqslant 2$, there are seven partial waves possible, each corresponding to a given initial and final state with all angular momentum quantum numbers given. Using the usual nomenclature [22], these amplitudes are

$$
\begin{aligned}
a_0&: {}^1S_0\to {}^3S_1,\ \ l_\pi=1,\\
a_1&: {}^3P_1\to {}^3S_1,\ \ l_\pi=0,\\
a_2&: {}^1D_2\to {}^3S_1,\ \ l_\pi=1,\\
a_3&: {}^3P_1\to {}^3S_1,\ \ l_\pi=2,\\
a_4&: {}^3P_2\to {}^3S_1,\ \ l_\pi=2,\\
a_5&: {}^3F_2\to {}^3S_1,\ \ l_\pi=2,\\
a_6&: {}^3F_3\to {}^3S_1,\ \ l_\pi=2.
\end{aligned}
\tag{1}
$$

Very close to threshold, only s-wave pions are produced, and a single amplitude (a_1) is sufficient to describe the reaction. Slightly above threshold, the p-wave a_2 becomes significant, while the other p wave (a_0) remains small and is often neglected entirely. Among the d-wave amplitudes, at, for instance, 400 MeV, a_6 is the largest, followed by a_4, a_3, and a_5 with a factor of 20 between a_5 and a_6. This is known indirectly from partial-wave analyses [13,14] of angular distributions of cross section and analyzing power. The spin correlation data presented here offer a more direct study of the d-wave strength in $pp\to d\pi^+$. In order to demonstrate this, we need to express the observables in terms of the seven partial-wave amplitudes [Eq. (1)]. This has previously been done for the cross section and the analyzing power [23]. For the spin correlation coefficients, we find analogously

$$
\begin{aligned}
\frac{d\sigma}{d\Omega}=\frac{1}{16\pi}[&a_0^2+a_1^2+a_2^2+C_1+(a_2^2-2\sqrt{2}\,\mathrm{Re}(a_0a_2^*)\\
&+B_1+C_2)P_2^0(\cos\theta)+C_3P_4^0(\cos\theta)],
\end{aligned}
\tag{2}
$$

$$\frac{d\sigma}{d\Omega}(A_{xx}+A_{yy})=\frac{1}{16\pi}[-2a_0^2-2a_2^2+C_4 + (-2a_2^2+4\sqrt{2}\,\mathrm{Re}(a_0a_2^*) + C_5)P_2^0(\cos\theta)+C_6P_4^0(\cos\theta)], \quad (3)$$

$$\frac{d\sigma}{d\Omega}(A_{zz})=\frac{1}{16\pi}[-a_0^2+a_1^2-a_2^2+C_1-C_4 + (-a_2^2+2\sqrt{2}\,\mathrm{Re}(a_0a_2^*)+B_1+C_2-C_5) \times P_2^0(\cos\theta)+(C_3-C_6)P_4^0(\cos\theta)], \quad (4)$$

$$\frac{d\sigma}{d\Omega}(A_{xx}-A_{yy})=\frac{1}{16\pi}[(B_2+C_1)P_2^2(\cos\theta)+C_8P_4^2(\cos\theta)], \quad (5)$$

with $d\sigma/d\Omega$ being the unpolarized differential cross section. The observables in Eqs. (2)–(5) are functions of the center-of-mass reaction angle, θ, and the functions $P_l^m(\cos\theta)$ are the usual Legendre polynomials. In the above equations, the terms B_n are caused by interference between *s* and *d* waves and are given by a sum of terms $\mathrm{Re}(a_1a_i^*)(i=3,4,5,6)$, weighted by numerical factors which follow from angular momentum coupling. The terms C_n contain *d* waves only, i.e., a sum of a_i^2 and $\mathrm{Re}(a_ia_k^*)$ $(i,k=3,4,5,6)$, again weighted by the appropriate numerical factors. A derivation of Eqs. (2)–(5) can be found in Ref. [24].

From Eq. (5) one sees that the combination $A_{xx}-A_{yy}$ vanishes at all angles when there are no *d* waves. A departure from this behavior would be caused by an interference between *s* and *d* waves. It is also easy to see from Eqs. (2)–(4) that for all reaction angles, the following holds:

$$A_{zz}-A_{xx}-A_{yy}=1-\delta, \quad (6)$$

where δ contains only C_n terms, i.e., only *d*-wave amplitudes.

Thus, both quantities, $A_{xx}-A_{yy}$ and $A_{zz}-A_{xx}-A_{yy}-1$ are a direct measure of *d*-wave contributions. Clearly, $A_{xx}-A_{yy}$ provides a more sensitive test because here *d* waves interfere with the dominant a_1 amplitude.

VI. FINAL DATA AND COMPARISON WITH THEORY

We compare our data to the two newest, published phase shift solutions, namely SP96 the published partial-wave analysis of the VPI group [25]; range of validity 0–500 MeV, where the quoted energy is the laboratory energy of the pion in $\pi^+d\to pp$; and BU93 the published partial-wave analysis of the VPI group and Bugg [26]; range of validity 9–256 MeV.

Numerical values for both phase shift analyses have been obtained from the SAID interactive program [14]. As can be seen from Fig. 1, our data are in good agreement with both phase shift solutions, although the agreement with SP96 (overall $\chi^2=0.90$) is better than with BU93 (overall $\chi^2=1.29$). As a function of energy we have $\chi^2=0.90$, 0.87, 0.99 (SP96), and $\chi^2=1.64$, 0.88, 1.50 (BU93) at 350.5, 375.0, and 400.0 MeV, respectively. This indicates that the energy dependence of SP96 near threshold is slightly closer to the data. Also shown in Fig. 1 are the A_{zz} data of Ref. [12] which agree with our data.

The quantity $A_{xx}-A_{yy}$ provides a sensitive and direct test of *d*-wave contributions in $\vec{p}\vec{p}\to d\pi^+$. Our data are consistent with negligible *d*-wave contributions even at 400 MeV (see Fig. 1).

VII. SUMMARY

In summary, we have measured the analyzing power and spin correlation coefficients in $\vec{p}\vec{p}\to d\pi^+$. The spin correlation coefficients allow a direct determination of *d*-wave contributions. In particular, $A_{xx}-A_{yy}$ provides a sensitive test because here *d* waves interfere with the dominant a_1 amplitude. Our data are consistent with negligible *d*-wave contributions even at 400 MeV. In addition, our data are well described by a partial wave solution (SP96) of the Virginia group.

ACKNOWLEDGMENTS

We are grateful for the untiring efforts of the accelerator operations group at IUCF, in particular G. East and T. Sloan. This work was supported in part by the National Science Foundation and the Department of Energy. This work has been supported by the U.S. National Science Foundation under Grant Nos. PHY-9602872, PHY-9901529, PHY-9722556, and by the U.S. Department of Energy under Grant No. DE-FG02-88ER40438.

APPENDIX

Since Mandl and Regge [22] introduced their nomenclature to describe the reaction $\vec{p}\vec{p}\to d\pi^+$, several different notations for the observables have been in use. We have been adhering to the notation of the Madison Convention [27] for the polarization observables, i.e., analyzing powers and spin correlation coefficients are labeled A_i and A_{ij} where $i,j=x,y,z$. The positive *z* axis is along the direction of momentum of the incident particle. In order to facilitate easy reading and comparison with the literature, we relate our observables to the notation of Niskanen [28]. The following equations have been obtained using Table I of Ref. [28]:

$$\frac{\sigma_{y0}}{\sigma_{00}}=\cos\phi A_y^b, \quad (A1)$$

$$\frac{\sigma_{0x}}{\sigma_{00}}=-\sin\phi A_y^t, \quad (A2)$$

$$\frac{\sigma_{yy}}{\sigma_{00}} = \sin^2\phi A_{xx} + \cos^2\phi A_{yy}, \tag{A3}$$

$$\frac{\sigma_{yx}}{\sigma_{00}} = \sin\phi\cos\phi(A_{xx} - A_{yy}), \tag{A4}$$

$$\frac{\sigma_{yz}}{\sigma_{00}} = \sin\phi A_{xz}, \tag{A5}$$

$$\frac{\sigma_{zz}}{\sigma_{00}} = A_{zz}. \tag{A6}$$

Here, σ_{00} is the unpolarized differential cross section and ϕ is the azimuthal angle of the pion. Furthermore, Niskanen uses P_B and P_T for beam and target polarization where we use P and Q, respectively.

[1] P. Heimberg *et al.*, Phys. Rev. Lett. **77**, 1012 (1996).
[2] D. Drochner *et al.*, Phys. Rev. Lett. **77**, 454 (1996).
[3] E. Korkmaz *et al.*, Nucl. Phys. **A535**, 637 (1991).
[4] H. O. Meyer *et al.*, Nucl. Phys. **A539**, 633 (1992).
[5] W. W. Daehnick *et al.*, Phys. Rev. Lett. **74**, 2913 (1995).
[6] J. G. Hardie *et al.*, Phys. Rev. C **56**, 20 (1997).
[7] W. W. Daehnick *et al.*, Phys. Lett. B **423**, 213 (1998).
[8] R. W. Flammang *et al.*, Phys. Rev. C **58**, 916 (1998).
[9] H. O. Meyer *et al.*, Phys. Rev. Lett. **81**, 3096 (1998).
[10] Swapan K. Saha *et al.*, Phys. Lett. B **461**, 175 (1999).
[11] H. O. Meyer *et al.*, Phys. Rev. Lett. **83**, 5439 (1999).
[12] E. Aprile-Giboni *et al.*, Nucl. Phys. **A431**, 637 (1984).
[13] D. V. Bugg, J. Phys. G **10**, 47 (1984).
[14] The SAID dial-in: available via TELNET to clsaid.phys.vt.edu, with userid:said (no password required).
[15] K. M. Watson, Phys. Rev. **88**, 1163 (1952).
[16] T. Wise, A. D. Roberts, and W. Haeberli, Nucl. Instrum. Methods Phys. Res. A **336**, 410 (1993).
[17] T. Rinckel *et al.*, Nucl. Instrum. Methods Phys. Res. A **439**, 117 (2000).
[18] F. Rathmann *et al.*, Phys. Rev. C **58**, 658 (1998).
[19] B. Lorentz *et al.* (unpublished).
[20] B. v. Przewoski *et al.*, Phys. Rev. C **58**, 1897 (1998).
[21] H. O. Meyer, Phys. Rev. C **56**, 2074 (1997).
[22] F. Mandl and T. Regge, Phys. Rev. **99**, 1478 (1955).
[23] C. L. Dolnick, Nucl. Phys. **B22**, 461 (1970).
[24] L. D. Knutson, in Proceedings of the 4th International Conference on Nuclear Physics at Storage Rings, Bloomington, 1999, edited by H. O. Meyer and P. Schwandt, AIP Conf. Proc. (AIP, Melville, NY, in press).
[25] C. H. Oh *et al.*, Phys. Rev. C **56**, 635 (1997).
[26] R. A. Arndt *et al.*, Phys. Rev. C **48**, 1926 (1993).
[27] Madison Convention, *Proceedings of the 3rd International Symposium on Polarization Phenomena in Nuclear Reactions*, edited by H. H. Barschall and W. Haeberli (University of Wisconsin, Madison, 1970), p. XXV.
[28] J. Niskanen, in *Polarization Phenomena in Nuclear Physics*, Proceedings of the 5th International Symposium on Polarization Phenomena in Nuclear Reactions, 1980, edited by G. Ohlsen *et al.*, AIP Conf. Proc. No. 69 (AIP, New York, 1981), p. 62.